Temperature dependent thermoelectric transport in PEDOT– PSS conducting polymer: The effect of additives

Anthony Rohmer ⁽ⁱ⁾; Yves Lansac ⁽ⁱ⁾; Yun Hee Jang ⁽ⁱ⁾; Patrice Limelette ^{II}



J. Appl. Phys. 137, 015501 (2025) https://doi.org/10.1063/5.0242275





Articles You May Be Interested In

Thermoelectric properties of flexible PEDOT/PU and PEDOT/PVDF films

AIP Conf. Proc. (July 2019)

A simple green route to blue thermoelectric PEDOT: PSS

Appl. Phys. Lett. (December 2021)

AIP
Publishing

PEDOT: PSS/PEDOT composite film for high performance electrochemical electrode

AIP Conference Proceedings (January 2017)





Journal of Applied Physics

Special Topics Open
for Submissions

Learn More

Temperature dependent thermoelectric transport in PEDOT-PSS conducting polymer: The effect of additives

Cite as: J. Appl. Phys. 137, 015501 (2025); doi: 10.1063/5.0242275 Submitted: 3 October 2024 · Accepted: 9 December 2024 · Published Online: 2 January 2025

















- ¹Université de Tours, CNRS, GREMAN UMR 7347, Parc de Grandmont, 37200 Tours, France
- ²Laboratoire de Physique des Solides, CNRS UMR 8502, Université Paris-Saclay, 91405 Orsay, France
- Department of Energy Science and Engineering, DGIST, Daegu 42988, South Korea

ABSTRACT

We report on both the electrical and thermoelectric transport properties as a function of temperature in poly(3,4-ethylene dioxythiophene) (PEDOT)-poly(styrene sulfonate) conducting polymers for a wide range of dimethyl sulfoxide (DMSO) additives. Whereas an insulatinglike electrical behavior is found over the whole temperature range, a metallic-like thermopower is mainly observed. We show that the § resistivity appears to be governed by a three-dimensional variable range hopping mechanism due to disordered regions with a decreasing 💆 resistivity appears to be governed by a unree-unitensional variable range normal increasing scaling factor ρ_0 as a function of the DMSO ratio. The correlation between T_0 and ρ_0 demonsional variable range normal variable range normal variables. strates that they are both controlled by the localization length ξ_0 , which is strongly enhanced by the DMSO in agreement with the morphostrates that they are both controlled by the localization length ξ_0 , which is strongly enhanced by the DMSO in agreement with the morphological evolution of the PEDOT chains with the additive. On the other hand, the high-T positive metallic-like thermopower seems rather ξ_0 unaffected by the additive in contrast to its low-T counterpart, which appears negative below a characteristic temperature T_{switch} . By showing $\hat{\aleph}$ that the latter is closely related to the localization temperature, we propose to ascribe this sign switch to the thermoelectric contribution originating from disordered regions, which competes with the metallic ones due to ordered domains. While still controlled by the localization temperature, this negative contribution appears to be consistent with a phonon-drag component with a scaling behavior as T_0T^{-3} . These analyses allow us to discuss the overall temperature dependent thermoelectric properties in a consistent way by considering a heterogeneous structure with both ordered and disordered domains. By relating explicitly the electrical resistivity to the thermopower, our results do not only reconcile these transport coefficients, but they also provide a unified picture of the properties of the conducting polymers.

© 2025 Author(s). All article content, except where otherwise noted, is licensed under a Creative Commons Attribution (CC BY) license (https://creativecommons.org/licenses/by/4.0/). https://doi.org/10.1063/5.0242275

I. INTRODUCTION

By offering a unique combination of properties not available from any other known materials, the conducting polymers^{1,2} have now demonstrated their interest in a wide variety of applications. They can be used in organic photovoltaic³ and thermoelectric devices, as well as for bioelectronic purposes due to their flexibility.^{5,6} Among them, the poly(3,4-ethylene dioxythiophene)-poly (styrene sulfonate) (PEDOT-PSS) is one of the most prominent conducting polymers due to its outstanding electrical properties, chemical stability, biocompatibility, and commercial availability. As a matter of fact, it has been shown for instance that by fine-tuning the doping in PEDOT-PSS, namely, the charge carriers concentration, its thermoelectric performance⁸ could compete with the ones measured in inorganic compounds. Its thermoelectric performance has even exceeded the one previously measured in the parent polymer PEDOT-Tos according to the pioneering work of Bubnova et al.9 This highlights the versatility of its transport properties by stressing the importance of the influence of the solvents (additives) used during its processing 10-15 as well as the following posttreatments. 15,16 Nevertheless, most of the performed investigations have been focused on room temperature properties, which do not allow a full understanding of the underlying mechanisms. 17,18 As a consequence of this lack of temperature dependent measurements,

a) Author to whom correspondence should be addressed: patrice.limelette@univ-tours.fr

the interpretation and then the origin of their transport properties are in particular still under debate. This also results from the influence of the complex structure of the conducting polymers on their properties. 19,20 Instead of being fully crystalline 21 or amorphous 22 materials, they are actually considered to be semicrystalline, 23,24 namely, with crystallites (ordered regions) more or less connected together and embedded in amorphous regions. Therefore, various transport models have been proposed in order to describe their properties, ranging from hopping-like by assuming localized charge carrito metallic-like by considering nearly or fully delocalized ones. 26,27 The former models account for the insulating-like temperature dependence of the electrical conductivity usually observed for instance, whereas the latter ones are able to describe the metallic-like T-dependence of the thermopower^{28,29} and its scaling properties. On the other hand, distinct approaches have been proposed following the pioneering ideas of Kaiser, 19,29,31 which consist in considering the conducting polymers as a heterogeneous medium with highly conducting (metallic) crystalline regions connected by less conducting (insulating) disordered ones.^{33,34} Whereas the original Kaiser model^{19,33} requires the use of unknown form factors, which limit the quantitative analysis of the transport properties, the recently introduced Heterogeneous Oriented Structure (HOSt) model succeeds in overcoming this difficulty.³⁴ Originally introduced in order to account for the thermoelectric transport properties in highly oriented conducting polymers, it has also demonstrated its wide applicability to non-oriented ones by considering an effective heterogeneous medium. This model consists in introducing three parameters in order to describe the complex structure of the polymers with the crystallinity, the preferred orientation of the ordered regions and their anisotropy. The crystallinity accounts for the proportion of ordered or crystalline domains and is then defined as the ratio between the volume of the ordered regions and the total one. It can vary from 0 in the case of completely amorphous polymer up to 1 if it is perfectly crystallized. The preferred orientation of the domains is originally related to the experimental method used to align the ordered domains such as the high temperature rubbing.3 This leads to introduce an alignment factor γ , which accounts for the degree of orientation along the rubbing direction. Thus, $\gamma = 1$ if the ordered domains are parallel to the latter direction and the measurements are performed along with, and $\gamma = 0$ for perpendicular measurements. The anisotropy results from the quasi one-dimensional molecular structure of the polymer backbone, which should influence the charge transport depending on the stacking of the chains in the ordered domains. It has been necessary to describe quantitatively the transport properties measured in highly oriented polymers. The introduction of the crystallinity ratio and the alignment degree allows to remove the unknown geometrical factor in such an heterogeneous model and then to relate the experimentally inferred transport coefficients to those characterizing both ordered and disordered domains. Interestingly, it has been shown that non-oriented conducting polymers could also be described according to the HOSt model by considering an effective heterogeneous medium with an intermediate alignment degree such as $\gamma = 1/2$. This means that the random distribution of the domains orientation can be projected onto both oriented configurations, namely, parallel and perpendicular. In other words, the non-oriented conducting polymer is then considered a parallel oriented one connected in series to a perpendicular one.

So here, we report on the temperature dependence of the thermoelectric transport properties, both electrical conductivity (or resistivity) and thermopower, in PEDOT-PSS thin films by varying the amount of solvent added prior to the deposition. We analyze our results first independently by inferring microscopic quantities and then try to correlate them in order to discuss their consistency in the general frame of the HOSt model and then to improve our understanding of their thermoelectric properties.

II. EXPERIMENTAL

The investigated conducting polymers are all made from the mixing of commercial PEDOT-PSS (Clevios PH1000) with anhydrous dimethyl sulfoxide (DMSO, Sigma-Aldrich). The PEDOT-PSS is a blend of two distinct polymers with the PEDOT, which is a conducting conjugated polymer, while the PSS is an insulating polymer with a styrene backbone and a sulfonate group allowing the solubility of the blend and acting as the PEDOT counterpart dopant. The PEDOT-PSS has an entangled-like chain structure leading to an heterogeneous film morphology with crystallized grains and amorphous regions depending on the processing conditions. The investigated PEDOT-PSS is actually known to allow to reach best electrical conductivity due to the ratio of PEDOT to PSS (1:2.5 w/w),³⁶ especially when solvents such as DMSO or ethylene glycol (EG) are added prior to the deposition for instance. Here, several volumes of DMSO have been added to PEDOT-PSS in order to prepare 1%, 2%, 3%, 4%, 5%, 6%, 7%, 8%, and 10% (v/v) solutions. The solutions were stirred for 1 h by 1000 rpm magnetic agitator and then the thin films were deposited in air by spin coating $20 \mu l$ of the solution on $9 \times 9 \,\mathrm{mm}^2$ pre-cleaned glass substrates. Prior to the spin coating, the substrates were first cleaned for 5 min in an ultrasonic isopropanol bath, then dried in forced-air oven, and, finally, treated in an argon plasma during 300 s in a Cressington sputter coater 108. Each film was spin coated at 4000 rpm for 60 s and finally dried 15 min at 150 °C on a hot plate. This procedure has yielded a reproducible thin film thickness of 53 (± 2) nm as checked with a dektak profilometer according several averaged measurements.

In order to allow thermoelectric measurements, gold electrodes have been deposited on the films through a mask, on which copper connectors have been silver pasted and dried on hot plate for 10 min at 130 $^{\circ}$ C.

The overall transport measurements have been performed using the standard four points method with a physical properties measurements system from Quantum Design. This method allows to measure both the electrical resistivity and thermopower as a function of temperature under high vacuum ($P < 10^{-5}$ mbar) by using a commercial Thermal Transport Option from Quantum Design. Note that such a vacuum is necessary to measure the only temperature dependence of the resistivity and not a combined effect of the pressure-temperature dependence, which should induce spurious behavior. Temperature rise of 3% has been applied in order to measure thermopower and electrical current of typically $10 \,\mu\text{A}$ has been used for resistivity measurements.

III. RESULTS AND DISCUSSION

We have measured the T-dependence of both the electrical resistivity ρ and the thermopower α from room temperature down

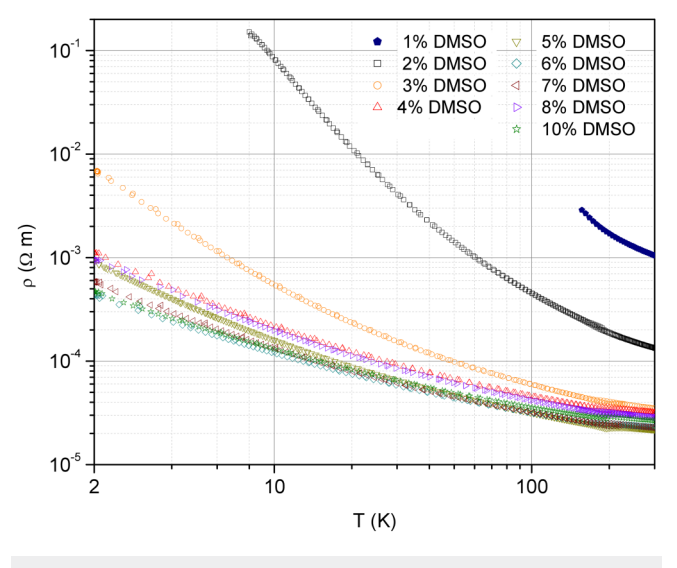


FIG. 1. Temperature dependence of the electrical resistivity measured in PEDOT-PSS for various DMSO ratios.

to 2 K for various DMSO ratios ranging from 1\% up to 10\%. As displayed in Fig. 1, the latter interval allows to broadly vary the magnitude of the resistivity over several decades. Despite this large effect, the observed T-dependence remains insulating-like with a decreasing resistivity as T increases whatever the DMSO content.

As already observed with DMSO or EG,15 the corresponding calculated electrical conductivity $\sigma = 1/\rho$ mainly increases in Fig. 2 at room temperature as a function of the additive content by revealing a maximum in between 5% and 7% up to roughly

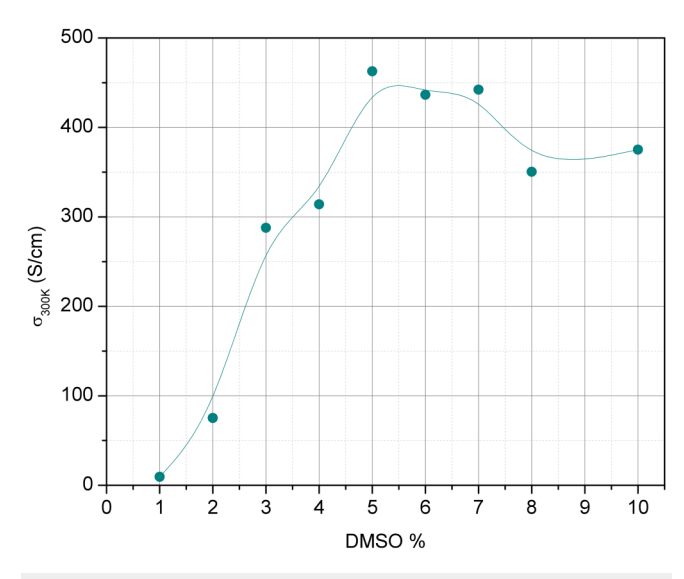


FIG. 2. Variation of the room temperature electrical conductivity measured in PEDOT-PSS as a function of the DMSO ratio.

500 S/cm, followed by a slight reduction. This kind of behavior is usually explained by the polarity of the additive, which can screen the coulombic interaction between the PSS chains and the PEDOT ones. As a result, the morphology of the PEDOT chains is altered by enabling a better packing, and it has also been suggested that a consecutive change from the benzoid to quinoid structure favors a more linear structure and then a more conducting polymer.^{37–41} If too much solvent is added, one can assume that a new kind of disorder is introduced, which leads to a decrease in conductivity as observed for DMSO ratios higher than 7%.

On the other hand, the temperature dependence of the measured electrical resistivity in Fig. 1 can be further analyzed. Actually, by plotting $\ln{(\rho/\rho_0)}$ in Fig. 3 as a function of the reduced temperature as $(T_0/T)^{1/4}$ for the various investigated DMSO ratios, the overall results can be scaled onto a single curve. This demonstrates that the electrical transport is fully governed by a variable range hopping (VRH) process, which is a typical signature of an electronic conduction in a disordered medium.

Originally introduced by Mott, this kind of transport is characterized by an insulating-like behavior with a resistivity varying as $\rho=\rho_0\,e^{(T_0/T)^{1/(D+1)}}$, with the dimensionality of the transport D, the localization temperature T_0 , and the scaling factor ρ_0 . Here, T_0 represents somehow an energy related to energetic fluctuations induced by the disorder, which localizes the electronic wave functions over a typical distance known as the localization length ξ_0 . The higher the localization temperature, the shorter the localization length. According to the found scaling in Fig. 3, the electronic transport is here consistent with a three-dimensional VRH.

Furthermore, both the localization temperature and the scaling factor can then be plotted as a function of the DMSO ratio $\frac{14}{13} - \frac{1}{\rho = \rho_0} \exp((T_0/T)^{1/4})$

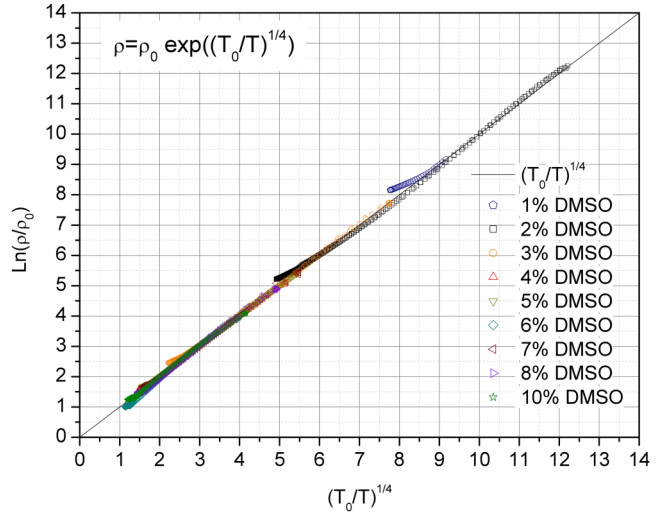


FIG. 3. Scaling of the measured electrical resistivity as $\ln(\rho/\rho_0)$ as a function of the reduced temperature as $(T_0/T)^{1/4}$ for various DMSO ratios, with the localization temperature T_0 and the scaling parameter ρ_0 . The overall scaling demonstrates that the electrical transport is governed by a three-dimensional variable range hopping mechanism.

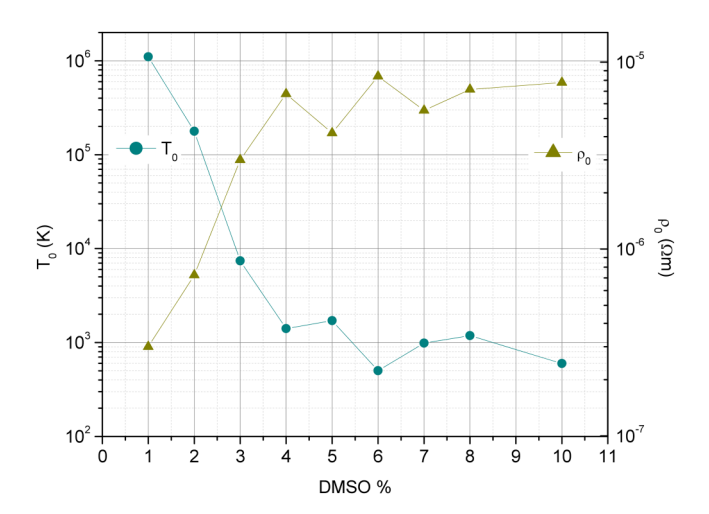


FIG. 4. Variations of the localization temperature T_0 (left axis) and the scaling parameter ρ_0 as a function of the DMSO ratio.

in Fig. 4, respectively, on the left and the right axis. The former displays a huge decrease from nearly 2 × 10⁵ K (2% DMSO) down to 500 K (6% DMSO), or equivalently in terms of energy from 15 eV down to 43 meV. Note that the localization temperature found for the sample with 1% DMSO is even higher but less well-defined due to the high electrical resistance measured for this DMSO ratio. These values illustrate the strong reduction of the disorder induced by the PSS chains due to the DMSO addition according the aforementioned screening mechanism. Interestingly, it is worthy to note that whereas the former T_0 is of the same order of magnitude than typical electronic binding energies, the latter one is only twice the value of the room temperature. This means that such a disorder could nearly be screened by thermal fluctuations at 300 K and thus that the electrons are at the edge of delocalization for a DMSO ratio of 6%.

At the contrary, the right axis in Fig. 4 shows a significant increase of the scaling factor ρ_0 , which can be thought of as a minimum resistivity theoretically reached if T goes to infinity. The observed tendency suggests that there is an asymptotic saturation value which could be of the order of $1 \text{ m}\Omega\text{cm}$, namely, the same one as the minimum for a metallic conductivity. This seems to agree with the previous comment that the polymer is in a regime very close to metallicity.

On the other hand, the increase of ρ_0 with the DMSO ratio can appear surprising but actually, it could be explained rather straightforwardly if one admits that it is controlled by the localization length. This assumption can in fact be checked by plotting in Fig. 5 this scaling factor as a function of the localization temperature. By doing so, the log-log scale allows to evidence a rather welldefined power law $\rho_0 \propto T_0^{-1/3}$. Since the localization temperature can be written such as $k_B T_0 \sim 1/(g(E_F)\xi_0^3)$, with the Boltzmann constant k_B and the density of states at the Fermi level $g(E_F)$, the power law observed in Fig. 5 simply suggests that $\rho_0 \propto \xi_0$. Therefore, the variation displayed in Fig. 4 could also represent the variation of the localization length as a function of the DMSO ratio

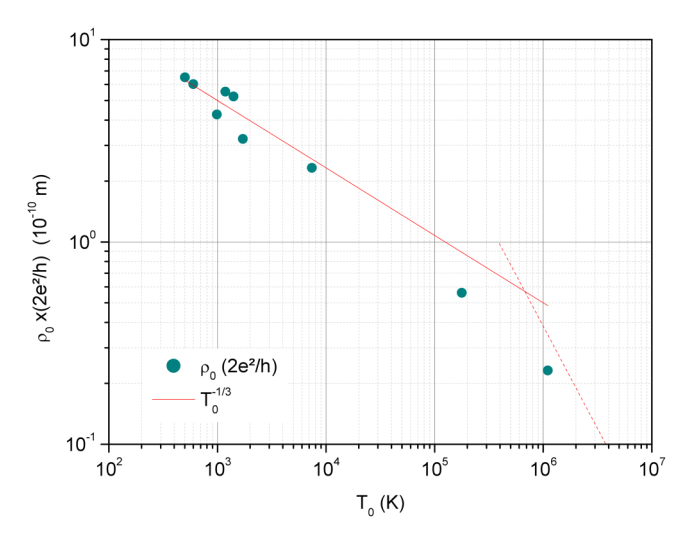


FIG. 5. Variation of the scaling parameter ho_0 here defined as a length by multiplying it by the quantum of conductance $2e^2/\hbar$, with the elementary charge e and the Planck constant h, as a function of the localization temperature T_0 . While the localization temperature is expected to vary as ξ_0^{-3} , with the localization length ξ_0 , the observed variation $\rho_0 \sim T_0^{-1/3}$ strongly suggests that ρ_0 is proportional to ξ_0 . Whereas the red line is a fit varying as $T_0^{-1/3}$, the dotted line indicates a power law as T_0^{-1} as it could be expected for one-dimensional VRH.

with first a large increase favoring the conduction process up to a saturation value suggesting that above typically 5%, the DMSO content itself could limit the delocalization.

It follows that the scaling factor plotted as a length in Fig. 5 by multiplying it by the quantum of conductance is actually proportional to the localization length. As a consequence, the variations of both T and a display of the T and a display of the transfer of both T and a display of the transfer of both T and a display of the transfer of both T and a display of the transfer of both T and a display of the transfer of both T and a display of the transfer of both T and a display of the transfer of both T and a display of the transfer tions of both T_0 and ρ_0 displayed in Fig. 4 result from the increase of the localization length with the DMSO ratio. Interestingly, a departure from the $T_0^{-1/3}$ behavior is observed when the localization temperature becomes very high, typically higher than 10⁵ K. Since the localization temperature is expected to vary as ξ_0^{-D} , with the dimensionality D, this could suggest some kind of dimensional crossover. As a matter of fact, it has already been reported that in the pristine PEDOT-PSS, namely, without additive, the resistivity varies as $\rho_0 e^{(T_0/T)^{1/2}}$ by suggesting that the transport becomes one-dimensional.⁴⁵ Therefore, the departure from the $T_0^{-1/3}$ behavior observed in Fig. 5 may prelude to a variation as T_0^{-1} shown by the dotted line because of such a dimensional crossover.

Now let us turn to the analysis of the thermopower, which is based on the overall temperature dependence displayed in Fig. 6. Whatever the DMSO ratio be, it appears continuously increasing with T, mainly positive over a wide temperature range but with a sign switch below a characteristic temperature, T_{switch} , strongly dependent on the additive content as it will be further discussed. With a room temperature value of the order of $12 \mu V/K$, it should also be noted that all the measured thermopowers are mainly superimposed as long as $T \gg T_{switch}$. This suggests that the DMSO additive does not significantly affect the positive-like thermopower in contrast to its negative counterpart.

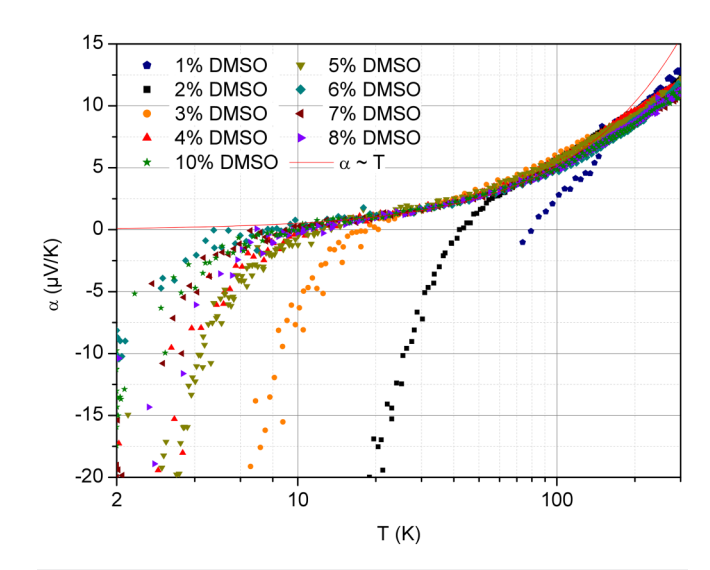


FIG. 6. Temperature dependence of the thermopower measured in PEDOT-PSS for various DMSO ratios. Whereas the thermopower is mainly positive over the whole temperature range, its sign switches to negative at low temperatures depending on the DMSO ratio by defining a characteristic temperature T_{switch} when α vanishes. The red line is the same linear fit as displayed in Fig. 7 and discussed in the text.

In order to better characterize its common positive part, the thermopower measured in the 6% DMSO sample is plotted in Fig. 7 in log-log scales as a function of temperature. It turns out that if $T > T_{switch}$, a rather well-defined linear behavior appears over one decade between 10 and 100 K, which is a typical signature

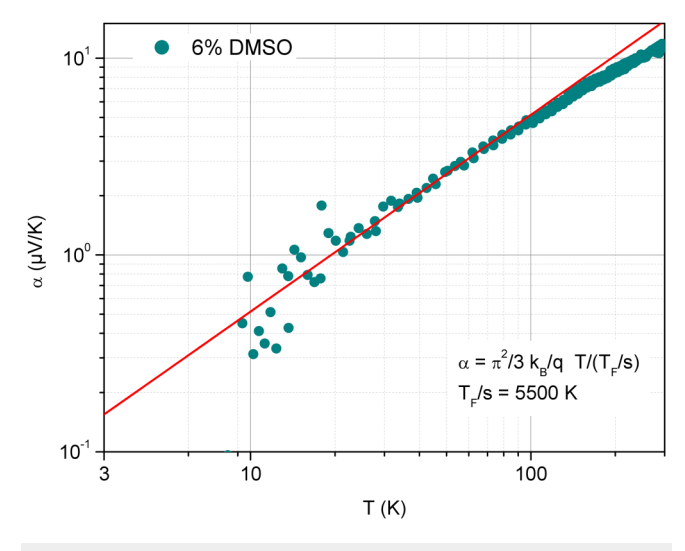


FIG. 7. Temperature dependence of the thermopower as measured in PEDOT-PSS with a 6% DMSO ratio. The log-log scales allow to identify a linear behavior between roughly 10 and 100 K consistent with a metallic contribution.

of a metallic contribution. Interestingly, it should be noted that such a metallic signature agrees with recent optical spectroscopy measurements performed in PEDOT-PSS. 46 This metallic thermopower can be further analyzed for instance in the frame of the so-called Mott formula as reminded in Eq. (1) with the energy dependent conductivity function $\sigma_E = q^2 \tau_E v_E^2 g_E$, with the elementary charge q, the relaxation time τ_E , the quasiparticles velocity ν_E , and the density of states g_E , where the subscript E indicates a possible energy dependence,

$$\alpha = \frac{\pi^2 k_B}{3} k_B T \left[\frac{\partial \ln (\sigma_E)}{\partial E} \right]_{E_F}.$$
 (1)

By assuming power law energy dependence such as $\tau_E \propto E^{\theta}$, $v_E^2 \propto E^{\nu}$, and $g_E \propto E^{\gamma_g}$ with the exponents θ , ν , and γ_g , it follows then a simple relation for the thermopower with the introduction below of the Fermi temperature as $E_F = k_B T_F$ and the sum of the exponents $s = \theta + v + \gamma_g$,

$$\alpha = \frac{\pi^2 k_B}{3} \frac{T}{q} \frac{T}{T_F/s}.$$
 (2)

Note that one recovers here the exponent s found in most of the conducting polymers when scaling the thermopower as a function of the electrical conductivity $(\alpha \propto \sigma^{-1/s})$ by varying the doping, 27 with usually s = 4. Anyway, Eq. (2) shows that the slope of the T-linear part of the thermopower in Fig. 7 is in principle $\underline{\omega}$ directly related to (T_F/s) which is proportional to the Fermi energy. directly related to (T_F/s) which is proportional to the Fermi energy. Here, the deduced Fermi temperature is $T_F/s \approx 5500 \, \mathrm{K}$ but a direct interpretation of its magnitude remains difficult at this stage since the analyzed contribution is metallic, whereas the electrical transport is insulating-like.

As observed in most conducting polymers, this apparent con-

tradiction can be removed by considering that these materials consist in an heterogeneous medium with ordered domains (crystallites or coherent aggregates) coexisting with disordered ones (amorphous regions). Early raised by Kaiser in particular, the heterogeneity of the conducting polymers makes the quantitative interpretation of the transport coefficients very tricky. Nevertheless, a recent theoretical framework has been proposed in order to address quantitatively this issue according to the so-called Heterogeneous Oriented Structure (HOSt) model. It has been first applied to highly oriented conducting polymers by considering parallel both ordered and³⁴ disordered domains with proportions described by a crystallinity ratio χ . Then, the introduction of an alignment degree γ allows to account for the orientation of these domains with respect to the current and temperature gradient. If $\gamma = 1$ (0), the domains are parallel (perpendicular) to the gradients. Furthermore, non-oriented conducting polymers can also be described by considering that the random distribution of the crystallites can be projected onto both oriented configurations, namely, parallel and perpendicular. This leads to an effective heterogeneous medium with an alignment degree $\gamma = 1/2$ which includes a parallel component connected in series to a perpendicular one, each of them being heterogeneous. In order to connect more deeply the alignment degree to the microscopic orientation of the crystallites,

it should be noted that the value $\gamma = 1/2$ represents the absence of preferred orientational order. The latter is usually related to a nematic-like order parameter⁴⁷ S with S = 1 and S = 0, which correspond, respectively, to the parallel orientation of the ordered domains (nematic phase) and to the random distribution of their orientation (isotropic phase). In three dimensions for instance, the nematic order parameter is given by $S_{3D} = \langle 3 \cos^2 \theta - 1 \rangle / 2$. Actually, such a definition results from the fact that a random orientational distribution in D dimensions (Appendix A) is characterized by $\langle \cos^2 \theta \rangle = 1/D$ and then that the nematic order parameter S_D should be proportional to $\langle D \cos^2 \theta - 1 \rangle$ in order to vanish in the isotropic phase. As a consequence, S_D must be normalized by (D-1) as $S_D=\frac{\langle D\cos^2\theta-1\rangle}{D-1}$ in order to fulfill $S_D=1$ in the nematic phase. It follows therefore that if D = 2 the nematic order parameter⁴⁸ will change as $S_{2D} = \langle 2 \cos^2 \theta - 1 \rangle = \langle \cos(2\theta) \rangle$. Interestingly, one recovers here that in the nematic phase with an angular orientational distribution defined with a Dirac function as $f(\theta) = \delta(\theta)$, the order parameter is $S_{2D} = 1$ and in the transverse nematic phase with an angular orientational distribution as $f(\theta) = \delta(\theta - \pi/2)$, the order parameter is $S_{2D} = -1$. In addition, it follows in the case of an in-plane random distribution with $f(\theta) = \frac{1}{\pi}$ that: $S_{2D} = \langle \cos(2\theta) \rangle = \int_0^{\pi} \cos(2\theta) f(\theta) d\theta = 0$. As a consequence, the alignment degree appears as a reformulation of the orientational order parameter in two dimensions as $\gamma = (S_{2D} + 1)/2$, with the correspondence between the parallel configuration ($\gamma = 1$) with the nematic phase ($\theta = 0$, $S_{2D} = 1$), the perpendicular one ($\gamma = 0$) with the transverse nematic phase $(\theta = \pi/2, S_{2D} = -1)$ and the non-oriented configuration ($\gamma = 1/2$) with the isotropic phase $(S_{2D} = 0)$. This description and the in-plane random orientation of domains is well supported by previously reported experimental results, which have shown that spin coated thin films was found to consist of horizontal layers of flattened PEDOT-rich particles randomly oriented.4

Therefore, the HOSt model allows to relate all the transport coefficients, the thermopower as well as the electrical and the thermal conductivities, as a function of those characterizing the ordered and the disordered domains according to the orientational order. Thus, it results that the transport coefficients as the electrical conductivity and the thermopower inferred from the HOSt model³⁴ can be explicitly related below to the effective nematic order parameter (Appendix B),

$$\sigma = \frac{2\sigma_{\parallel}\sigma_{\perp}}{(1 - S_{2D})\sigma_{\parallel} + (1 + S_{2D})\sigma_{\perp}},\tag{3}$$

$$\alpha = (1 + S_{2D}) \frac{\kappa}{2\kappa_{\parallel}} \alpha_{\parallel} + (1 - S_{2D}) \frac{\kappa}{2\kappa_{\perp}} \alpha_{\perp}. \tag{4}$$

Note that the definition of the thermal conductivity follows the electrical one. In addition, if the disordered domains resistivity (its perpendicular component $\rho_{\perp,dis}$ in the terminology of the HOSt model) is much higher than the ordered domains one, it can be shown that the measured ρ is mainly dominated by $\rho_{\perp,dis}$ as $\rho \approx (1-S_{2D})(1-\chi)\rho_{\perp,dis}/2=(1-\chi)\rho_{\perp,dis}/2$ with $S_{2D}=0$. This explains the insulating-like behavior observed in Fig. 1.

On the other hand, the thermopower is expected to be the sum of two components weighted by relative thermal conductivities.³⁴ If the ordered domains conduct much more than the disordered ones both heat and charge, one would then expect in the frame of the HOSt model that $\alpha \approx \frac{\kappa_{dis}}{\chi(1-\chi)\kappa_{ord}}\alpha_{ord} + \alpha_{dis}$ with here $S_{2D}=0$ and if the anisotropy is neglected. Since the positive part of thermopower appears in Fig. 6 mainly unaffected by the variation of the DMSO which strongly influences the disorder as demonstrated in Fig. 4, it seems likely in this high temperature (HT) regime that $\alpha_{HT} \approx \frac{\kappa_{dis}}{\chi(1-\chi)\kappa_{ord}}\alpha_{ord}$, κ_{dis} being essentially governed by the lattice-like contribution. This means that the disordered contribution to the thermopower seems negligible within this regime. Now, if the disordered domains thermal conductivity mimics the ordered domains one with a lower magnitude, the previous relation could explain the observed metallic linear temperature dependence in Fig. 7. This could be justified in this rather high temperature regime because the thermal conductivity of the ordered domains should be mainly given by their lattice contribution, the electronic component being a decreasing function of temperature. This also illustrates the difficulty to interpret quantitatively the found effective Fermi temperature since it is inferred from the slope, which involves a thermal conductivity ratio and the crystallinity. Nevertheless, the heterogeneity of the conducting polymers allows to reconcile the insulating-like electrical transport and the metallic-

Furthermore, one must emphasize that whereas it seems justified to neglect the disordered regions thermopower if α varies linearly with T, it appears no more valid at low temperatures when α turns out to be negative below T_{switch} . In contrast to the previously discussed regime, one expects at low temperatures that the thermal conductivity of the ordered domains should be given by the sum of & a lattice contribution $\kappa_{lat,ord}$ and an electronic component $\kappa_{el,ord}$ proportional to the corresponding electrical conductivity according to the Wiedemann-Franz law²¹ as $\kappa_{ord} = \kappa_{lat,ord} + \kappa_{el,ord}$. Since $\kappa_{el,ord}$ increases when T decreases, it can be assumed at low temperature (LT) that $\kappa_{ord} pprox \kappa_{el,ord} \gg \kappa_{dis}$. Then, it follows within this regime that the thermopower becomes governed by the disordered component as $\alpha_{LT} \approx \frac{\kappa_{dis}}{\chi(1-\chi)\kappa_{ord}} \alpha_{ord} + \alpha_{dis} \approx \alpha_{dis}$. This could explain the two distinct thermopower regimes observed in Fig. 6, with the positive mainly linear one related to the ordered domains and the negative one associated with the disordered regions. As a matter of fact, by plotting in Fig. 8, the temperature T_{switch} at which the thermopower vanishes as a function of the localization temperature deduced from the resistivity measurements, a correlation between both is unveiled such as $T_{switch} \propto T_0^{1/4}$. This behavior strongly suggests that the thermopower change of sign is related to the disordered domains.

Even if the positive metallic contribution is rather negligible at low temperature, it appears relevant to remove it from the measured thermopower in order to plot it as the positive quantity $-(\alpha-\alpha_{met})$, with $\alpha_{met}=\frac{\pi^2}{3}\frac{k_B}{q}\frac{T}{T_F/s}$ and the previously determined $T_F/s\approx 5500$ K. By doing so, the absolute value of the disordered component of the thermopower is then represented in Fig. 9 as a function of $T/T_0^{1/3}$. The normalization of the temperature by $T_0^{1/3}$ allows thus to scale this component whatever the DMSO content by demonstrating a power law variation such as $\alpha_{dis} \propto T_0/T^3$.

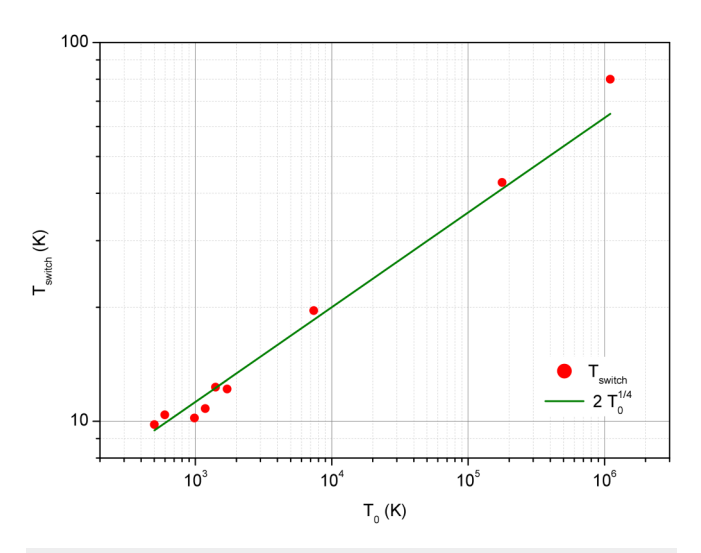


FIG. 8. Variation of the switch temperature T_{switch} as a function of the localization temperature T_0 . The observed behavior demonstrates a power law such as $T_{\text{switch}} \approx 2T_0^{1/2}$

Once more, this points out the influence of the disorder in this regime by making a direct correlation between the electrical conductivity and the low temperature thermopower in full agreement with the heterogeneous picture of the PEDOT-PSS as described in the frame of the HOSt model.

Furthermore, these results imply that the total thermopower can be written as $\alpha = \alpha_{met} + \alpha_{dis}$ with $\alpha_{met} = AT$ and $\alpha_{dis} = -BT_0/T^3$, A being a function of the effective Fermi

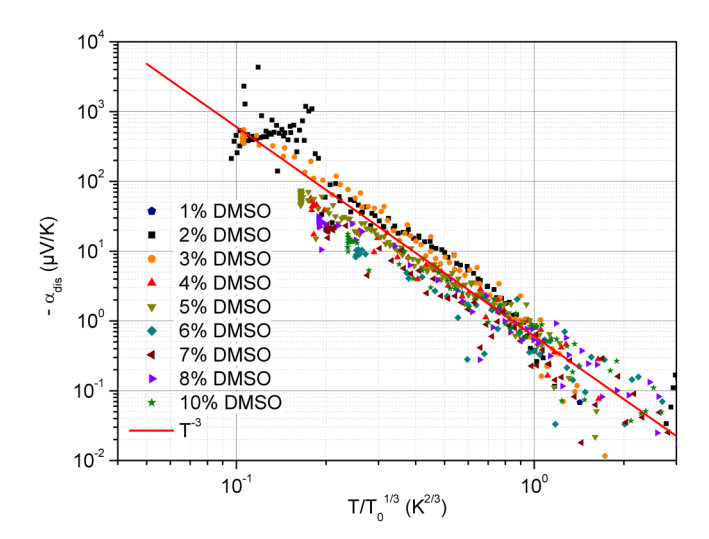


FIG. 9. Scaling of the disordered component of the thermopower as $-lpha_{
m dis}=-(lpha-lpha_{
m met})$, with $lpha_{
m met}=rac{\pi^2}{3}rac{R_{
m B}}{q}rac{T}{T_F/s}$, as a function of the temperature as $T/T_0^{1/3}$. This behavior demonstrates a variation as $\alpha_{dis} \propto T_0/T^3$, with the localization temperature To as shown in the red line.

temperature according to the Eq. (2) affected likely in magnitude by the thermal conductivity ratio as previously discussed. When α vanishes at the temperature T_{switch} , it follows then that α_{met} $=-\alpha_{dis}$ so $AT_{switch}=BT_0/T_{switch}^3$. Therefore, it results automatically that $T_{switch} = (B/A)^{1/4} T_0^{1/4}$ as previously observed in Fig. 8. This means that the overall temperature dependence of both α_{met} and α_{dis} fully agree with the power law behavior of T_{switch} as a function of the localization temperature T_0 inferred from the electrical conductivity. The high consistency of this analysis firmly demonstrates that the PEDOT-PSS must be considered as a heterogeneous material with both ordered (metallic) and disordered regions and that the HOSt model is a relevant paradigm in order to analyze its thermoelectric transport properties.

So finally, let us deeply discuss the observed low temperature dependence of the thermopower. One must first emphasize that in a VRH regime, the thermopower is expected to vary as $T^{(D-1)/(D+1)}$ with the dimensionality⁵⁰ D, which implies in particular that in three dimensions²² $\alpha \propto (T_0 T)^{1/2}$. This is clearly not observed here and the only contribution to our knowledge consistent with the found T^{-3} variation involves the so-called phonon-drag thermoelectric contribution.⁵¹ Basically, this effect results from the electron-phonon interaction, which relates the electric charge current to the heat current through the lattice leading, therefore, to an unusual thermoelectric behavior.5

At a phenomenological level, this can be related to the lattice heat flux density $\vec{J_O}$ induced by the electrostatic force density $ne\vec{E}$, with the electronic density n, the charge e, and the electric field \vec{E} . This force acts on the charges and works over a typical distance given by the phonon mean free path λ_{ph} . The phonons carrying thus an energy density of the order of $\|\lambda_{ph}ne\vec{E}\|$ with a velocity v_s , g_s the sound velocity, the resulting lattice heat flux density can be written as $\vec{J_Q} = v_s \lambda_{ph}ne\vec{E}$. On the other hand, according to this energy transfer the lattice heat flux density is also expected to be proportional to the current density $\vec{J_e} = ne\mu_{el}\vec{E}$, with the electronic mobility μ_{el} . The coefficient relating both flux densities being the Peltier coefficient Π_{phd} such as $\vec{J_Q} = \Pi_{phd}\vec{J_e}$, it follows then that $\Pi_{phd} = v_s \lambda_{ph}/\mu_{el}$. The so-called Kelvin relation between Π_{phd} and thermopower⁵¹ $\alpha_{phd} = \Pi_{phd}/T$ allows then to infer a phonon-drag contribution as $\alpha_{phd} = v_s \lambda_{ph}/(\mu_{el}T)$. Such a contribution has indeed been predicted in semiconductors for instance.⁵³ By considering the electronic mobility due to phonon scattering⁵² $\mu_{el} \propto T^{-3/2}$, the phonon-drag thermopower is expected to vary with temperature as $\alpha_{phd} \propto T^{1/2} \lambda_{ph}$, depending then on the phonon mean free path. The latter originates actually from a rather classical phonon picture since it is closely related to the lattice thermal conductivity $\kappa \approx 1/3 C_{\nu} v_s \lambda_{ph}$, with the lattice specific heat per unit volume C_{ν} . Nonetheless, the semi-classical lattice thermal conductivity can be considered in order to estimate λ_{ph} by using the proper scattering mechanism characterized by its energy dependent scattering time $\tau \propto \omega^{\theta_{ph}}$. It can be shown in this framework that the low temperature lattice thermal conductivity⁵⁴ varies as $\kappa \propto T^{3+\theta_{ph}}$, and then that the phonon mean free path behaves as $\lambda_{ph} \propto T^{\theta_{ph}}$ since $C_{\nu} \propto T^3$ according to the well known Debye law. Note that at very low temperature the so-called boundary regime

 $(\theta_{ph} = 0)$ is recovered with a thermal conductivity proportional to the specific heat, $\kappa \propto T^3$, since the phonon mean free path is limited by the sample size itself. Furthermore, by considering the impurity scattering mechanism which is usually relevant for the lattice thermal conductivity below 50 K and is characterized by $\theta_{ph} = -4$, one infers a phonon-drag thermopower contribution as $\alpha_{\it phd} \propto T^{1/2+\theta_{\it ph}} \propto T^{-3.5}$. This is already in good agreement with the power law T^{-3} observed in Fig. 9.

In fact, the previously deduced theoretical power law $T^{-3.5}$ can be refined by considering the phonon polarization and the crystal symmetry. 52,53 It has been demonstrated that an averaged phonon mean free path could behave as $\lambda_{ph} \propto T^{-(5-n/2)}$ with the exponent n varying typically between 2 and 4 depending on polarization and symmetry. It follows that the phonon-drag thermopower could vary as $\alpha_{phd} \propto T^{-(9-n)/2}$ leading thus to a temperature dependence between $T^{-3.5}$ and $T^{-2.5}$ in agreement with the $T^{-3.2}$ dependence previously observed in germanium⁵⁵ and the T^{-3} variation found here.

The fact that our results suggest besides a behavior as T_0T^{-3} is of course not predicted theoretically and is very likely a consequence of the variable range hopping regime, which takes place. One can here guess that due to this specific transport regime restricting the extension of the electronic wave functions over distances of the order of the localization length $\xi_0 \propto T_0^{-1/3}$, the electronic mobility entering in the definition of the phonon-drag thermopower could also be affected. For instance, it could seem reasonable to assume that the mobility could be proportional to the volume limited by ξ_0 , namely, ξ_0^3 , since this volume will restrict the area where the electrons could be scattered by phonons. This should imply that $\mu_{el} \propto \xi_0^3 \propto 1/T_0$ and then a thermopower contribution proportional to T_0 as observed. We believe, however, that this result calls for further theoretical investigations in order to carefully address this specific point.

On the other hand, we precise that even if the metallic part of the thermopower is weighted by the relative thermal conductivity, which lowers its contribution at low temperature, the combination of a phonon-drag component with a metallic one as α $=AT-BT_0/T^3$ is already sufficient to observe a linear high temperature behavior and a crossover at low temperatures toward a negative thermopower varying as T^{-3} . It should also be noted that thermopower sign changes have already been observed in other conducting polymers 56,57 such as the polyaniline for instance and have been interpreted by involving polaronic band effects. Since these previously reported sign changes vary very differently with temperature in comparison to the switch observed here, we believe that the suggested interpretations are not relevant in our case. Finally, one may emphasize that the negative phonon-drag contribution could suggest electron-like charge carriers in the disordered domains, but it is worth mentioning that the sign of such a contribution strongly depends on the complexity of the energy band structure, which prevents from drawing straightforward conclusion.5

IV. CONCLUSIONS

In order to summarize our work, we have investigated both the electrical and thermoelectric transport properties as a function of temperature in PEDOT-PSS conducting polymers for a wide range of DMSO additives. An insulating-like electrical behavior is found over the whole temperature range contrasting with the metallic-like thermopower mainly observed. We have shown that the resistivity appears governed by a three-dimensional variable range hopping mechanism due to disordered regions with a decreasing localization temperature T_0 and an increasing scaling factor ρ_0 as a function of the DMSO ratio. The correlation between T_0 and ρ_0 demonstrates that they are both controlled by the localization length ξ_0 , which is strongly enhanced by the DMSO in agreement with the morphological evolution of the PEDOT chains as expected with the additive. On the other hand, the high-T positive metallic-like thermopower seems rather unaffected by the additive in contrast to its low-T counterpart, which appears negative below a characteristic temperature T_{switch} . By showing that the latter is closely related to the localization temperature, we have proposed to ascribe this sign switch to the thermoelectric contribution originating from disordered regions, which competes with the metallic ones due to ordered domains. While still controlled by the localization temperature, the negative thermopower contribution appears consistent with a phonon-drag component with a scaling behavior as $T_0 T^{-3}$. By relating explicitly the electrical resistivity to the thermopower, our results do not only reconcile these transport coefficients, but they also provide a unified picture of the properties of the conducting polymers. The overall high consistency of these analysis demonstrates that the PEDOT-PSS must be considered as an heterogeneous material with both ordered (metallic) and disordered regions and that the HOSt model is a relevant paradigm in

order to analyze its thermoelectric transport properties.

ACKNOWLEDGMENTS

We acknowledge the Agence Nationale de la Recherche for financial support through the project THERMOPOLYS (No. 33 ANR-22-CF50-0020) and La Région Centre Val-de-Loire for financial support through the project THERMOPOLYS (No. 33 ANR-22-CF50-0020) and La Région Centre Val-de-Loire for financial support through the project THERMOPOLYS (No. 33 ANR-22-CF50-0020) and La Région Centre Val-de-Loire for financial support through the project THERMOPOLYS (No. 33 ANR-22-CF50-0020) and La Région Centre Val-de-Loire for financial support through the project THERMOPOLYS (No. 33 ANR-22-CF50-0020) and La Région Centre Val-de-Loire for financial support through the project THERMOPOLYS (No. 33 ANR-22-CF50-0020) and La Région Centre Val-de-Loire for financial support through the project THERMOPOLYS (No. 33 ANR-22-CF50-0020) and La Région Centre Val-de-Loire for financial support through the project THERMOPOLYS (No. 33 ANR-22-CF50-0020) and La Région Centre Val-de-Loire for financial support through the project THERMOPOLYS (No. 33 ANR-22-CF50-0020) and La Région Centre Val-de-Loire for financial support through the project THERMOPOLYS (No. 33 ANR-22-CF50-0020) and La Région Centre Val-de-Loire for financial support through the project THERMOPOLYS (No. 33 ANR-22-CF50-0020) and La Région Centre Val-de-Loire for financial support through the project THERMOPOLYS (No. 33 ANR-22-CF50-0020) and La Région Centre Val-de-Loire for financial support through the project THERMOPOLYS (No. 33 ANR-22-CF50-0020) and La Région Centre Val-de-Loire for financial support through the project THERMOPOLYS (No. 33 ANR-22-CF50-0020) and La Région Centre Val-de-Loire for financial support through the project THERMOPOLYS (No. 33 ANR-22-CF50-0020) and La Région Centre Val-de-Loire for financial support through the project THERMOPOLYS (No. 34 ANR-22-CF50-0020) and La Region Centre Val-de-Loire for financial support through the project through the project through the project through the ANR-22-CE50-0020) and La Région Centre Val-de-Loire for financial support through the project ETHERMO.

AUTHOR DECLARATIONS

Conflict of Interest

The authors have no conflicts to disclose.

Author Contributions

Anthony Rohmer: Investigation (equal); Methodology (lead); Writing - original draft (equal); Writing - review & editing (equal). Yves Lansac: Formal analysis (equal); Writing - original draft (equal). Yun Hee Jang: Formal analysis (equal); Writing original draft (equal). Patrice Limelette: Conceptualization (lead); Formal analysis (lead); Funding acquisition (lead); Investigation (equal); Project administration (lead); Writing - original draft (equal); Writing - review & editing (equal).

DATA AVAILABILITY

The data that support the findings of this study are available from the corresponding author upon reasonable request.

APPENDIX A: D-DIMENSIONAL NEMATIC ORDER **PARAMETER**

A nematic order parameter can be built in D dimensions by considering the following mean value for a random orientational distribution around the direction given by θ_1 ,

$$\begin{split} \langle \cos^2\theta_1 \rangle &= \frac{\int_0^\pi \cos^2\theta_1 \sin^{D-2}\theta_1 \, d\theta_1 \cdots \int_0^\pi \sin\theta_{D-2} \, d\theta_{D-2}}{\int_0^\pi \sin^{D-2}\theta_1 \, d\theta_1 \cdots \int_0^\pi \sin\theta_{D-2} \, d\theta_{D-2}} \\ &= \frac{\int_0^\pi \cos^2\theta_1 \sin^{D-2}\theta_1 \, d\theta_1}{\int_0^\pi \sin^{D-2}\theta_1 \, d\theta_1} \, . \end{split}$$

In the first line, the integrals over the angle θ_{D-1} , which ranges from 0 up to 2π have already been canceled out, and in the second one, the integrals over the angles θ_2 up to θ_{D-2} also. The following simplification can then be performed with the replacement $\cos^2\theta_1 = 1 - \sin^2\theta_1,$

$$\langle \cos^2 \theta_1 \rangle = 1 - \frac{\int_0^\pi \sin^D \theta_1 d\theta_1}{\int_0^\pi \sin^{D-2} \theta_1 d\theta_1} = 1 - \frac{I_D}{I_{D-2}}. \tag{A1}$$

Now, I_D can be related to I_{D-2} by performing an integration by

$$\begin{split} I_D &= \int_0^\pi \sin^D \theta_1 \, d\theta_1 = \int_0^\pi \sin^{D-1} \theta_1 \sin \theta_1 \, d\theta_1 \\ &= (D-1) \int_0^\pi \sin^{D-2} \theta_1 \cos^2 \theta_1 \, d\theta_1 \\ &= (D-1) \int_0^\pi \sin^{D-2} \theta_1 (1 - \sin^2 \theta_1) \, d\theta_1 \\ &= (D-1) (I_{D-2} - I_D). \end{split}$$

It results that $I_D = I_{D-2}(D-1)/D$ and according to Eq. (A1) that $\langle \cos^2 \theta_1 \rangle = 1/D$. As explained in the main text, the nematic order parameter must then be proportional to $D(\cos^2 \theta_1) - 1$ in order to vanish in the isotropic phase and be scaled by (D-1) as S_D $=\frac{D\langle\cos^2\theta_1\rangle-1}{D-1}$ in order to reach 1 in the nematic phase.

APPENDIX B: HOST MODEL TRANSPORT COEFFICIENTS

As shown in the main text, the relation between the alignment degree γ originally introduced³⁴ and the two-dimensional nematic order parameter S_{2D} allows to reformulate the transport coefficients according to Eqs. (3) and (4). However, these equations involve the transport coefficients defined in oriented configurations, parallel $(S_{2D} = 1)$ and perpendicular $(S_{2D} = -1)$, which also imply the contributions from both disordered and ordered domains as reminded thereafter. In particular, the electrical conductivity can be straightforwardly deduced in both configurations as

$$egin{aligned} \sigma_{\parallel} &= \chi \sigma_{ord,\parallel} + (1-\chi) \sigma_{dis,\parallel}, \ \sigma_{\perp} &= rac{\sigma_{ord,\perp} \sigma_{dis,\perp}}{(1-\chi) \sigma_{ord,\perp} + \chi \sigma_{dis,\perp}}. \end{aligned}$$

Note that the definition of the thermal conductivity follows the electrical one with the corresponding parameters. On the other hand, it has been shown³⁴ that the thermopower in the parallel configuration is a sum of two contributions originating from the disordered and ordered domains, each being weighted by the corresponding relative electrical conductivity,

$$egin{aligned} lpha_{\parallel} &= rac{\chi \sigma_{ord,\parallel}}{\chi \sigma_{ord,\parallel} + (1-\chi) \sigma_{dis,\parallel}} lpha_{ord,\parallel} \ &+ rac{(1-\chi) \sigma_{dis,\parallel}}{\chi \sigma_{ord,\parallel} + (1-\chi) \sigma_{dis,\parallel}} lpha_{dis,\parallel} pprox lpha_{ord,\parallel}. \end{aligned}$$

Since the electrical conductivity in the ordered domains is expected to be much higher than in the disordered domains, one recovers here that the thermopower in the parallel configuration is mainly given by the one from the ordered regions. The result is quite different in the perpendicular configuration because the contributions are now weighted by the inverse relative thermal conductivity as displayed below:

$$egin{align} lpha_{\perp} &= rac{\chi \kappa_{dis,\perp}}{\chi \kappa_{dis,\perp} + (1-\chi) \kappa_{ord,\perp}} lpha_{ord,\perp} \ &+ rac{(1-\chi) \kappa_{ord,\perp}}{\chi \kappa_{dis,\perp} + (1-\chi) \kappa_{ord,\perp}} lpha_{dis,\perp} \ &pprox rac{\chi \kappa_{dis,\perp}}{(1-\chi) \kappa_{ord,\perp}} lpha_{ord,\perp} + lpha_{dis,\perp}. \end{align}$$

In order to justify the last line, it should be noted that the thermal conductivity involves a lattice-like component and even if one should expect that $\kappa_{lat,ord} > \kappa_{lat,dis}$, the difference in magnitude should not be as large as for the electrical conductivity $(\sigma_{ord}\gg\sigma_{dis})$. This result demonstrates then that a contribution from the disordered domains can be expected if the contribution α_{\perp} survives, as it is the case in non-oriented polymers.

REFERENCES

¹A. J. Heeger, A. G. MacDiarmid, and H. Shirakawa, Macromolecules 35(4), 1137-1139 (2002).

 ${\bf ^2}{\rm A.\ J.\ Heeger},$ "Semiconducting and metallic polymers: The fourth generation of polymeric materials," J. Phys. Chem. B **105**, 8475 (2001).

³M. Vezie *et al.*, "Exploring the origin of high optical absorption in conjugated

polymers," Nat. Mater. 15, 746–753 (2016).

B. Russ, A. Glaudell, J. J. Urban, M. L. Chabinyc, and R. A. Segalman, "Organic thermoelectric materials for energy harvesting and temperature control," Nat. Rev. Mater. 1, 16050 (2016).

⁵T. Someya, Z. Bao, and G. G. Malliaras, "The rise of plastic bioelectronics," Nature 540, 379 (2016).

⁶G. Prunet, F. Pawula, G. Fleury, E. Cloutet, A. J. Robinson, G. Hadziioannou, and A. Pakdel, "A review on conductive polymers and their hybrids for flexible

- and wearable thermoelectric applications," Mater. Today Phys. 18, 100402 (2021).
- ⁷Y. Huang, L. Tang, and Y. Jiang, "Chemical strategies of tailoring PEDOT:PSS for bioelectronic applications: Synthesis, processing and device fabrication," CCS Chem. 6, 1844–1867 (2024).
- ⁸G. H. Kim, L. Shao, K. Zhang, and K. P. Pipe, "Engineered doping of organic semiconductors for enhanced thermoelectric efficiency," Nat. Mater. 12, 719–723 (2013).
- ⁹O. Bubnova, Z. U. Khan, A. Malti, S. Braun, M. Fahlman, M. Berggren, and X. Crispin, "Optimization of the thermoelectric figure of merit in the conducting polymer poly(3,4-ethylenedioxythiophene)," Nat. Mater. 10, 429 (2011).
- polymer poly(3,4-ethylenedioxythiophene)," Nat. Mater. 10, 429 (2011).

 10 L. A. A. Pettersson, S. Ghosh, and O. Inganäs, "Optical anisotropy in thin films of poly(3,4-ethylenedioxythiophene)–poly(4-styrenesulfonate)," Org. Electron. 3, 143–148 (2002).
- ¹¹J. Y. Kim, J. H. Jung, D. E. Lee, and J. Joo, "Enhancement of electrical conductivity of poly(3,4-ethylenedioxythiophene)/poly(4-styrenesulfonate) by a change of solvents," Synth. Met. **126**, 311–316 (2002).
- ¹²W. H. Kim, A. J. Mäkinen, N. Nikolov, R. Shashidhar, H. Kim, and Z. H. Kafafi, "Molecular organic light-emitting diodes using highly conducting polymers as anodes," Appl. Phys. Lett. **80**, 3844–3846 (2002).
- polymers as anodes," Appl. Phys. Lett. **80**, 3844–3846 (2002).

 13 S. K. M. Jönsson, J. Birgerson, X. Crispin, G. Greczynski, W. Osikowicz, A. W. Denier van der Gon, W. R. Salaneck, and M. Fahlman, "The effects of solvents on the morphology and sheet resistance in poly(3,4-ethylenedioxythiophene)-polystyrenesulfonic acid (PEDOT-PSS) films," Synth. Met. **139**, 1–10 (2003).

 14 X. Crispin, S. Marciniak, W. Osikowicz, G. Zotti, D. A. W. van der Gon,
- ¹⁴X. Crispin, S. Marciniak, W. Osikowicz, G. Zotti, D. A. W. van der Gon, F. Louwet, M. Fahlman, L. Groenendaal, F. de Schryver, and W. R. Salaneck, "Conductivity, morphology, interfacial chemistry, and stability of poly (3,4-ethylene dioxythiophene)–poly(styrene sulfonate): A photoelectron spectroscopy study," J. Polym. Sci., Part B: Polym. Phys. 41, 2561–2583 (2003).
- ¹⁵Y. H. Kim, C. Sachse, M. L. Machala, C. May, L. Müller-Meskamp, and K. Leo, "Highly conductive PEDOT:PSS electrode with optimized solvent and thermal post-treatment for ITO-free organic solar cells," Adv. Funct. Mater. 21, 1076–1081 (2011).
- ¹⁶N. Kim, S. Kee, S. H. Lee, B. H. Lee, Y. H. Kahng, Y. R. Jo, B. J. Kim, and K. Lee, "Highly conductive PEDOT:PSS nanofibrils induced by solution-processed crystallization," Adv. Mater. 26, 2268–2272 (2014).
 ¹⁷H. Shi, C. Liu, Q. Jiang, and J. Xu, "Effective approaches to improve the elec-
- ¹⁷H. Shi, C. Liu, Q. Jiang, and J. Xu, "Effective approaches to improve the electrical conductivity of PEDOT:PSS: A review," Adv. Electron. Mater. 1, 1500017 (2015).
- ¹⁸N. A. A. Shahrim, Z. Ahmad, A. W. Azman, Y. F. Buys, and N. Sarifuddin, "Mechanisms for doped PEDOT:PSS electrical conductivity improvement," Mater. Adv. 2, 7118–7138 (2021).
- ¹⁹A. B. Kaiser, "Thermoelectric power and conductivity of heterogeneous conducting polymers," Phys. Rev. B 40, 2806–2813 (1989).
- ²⁰B. Sixou, N. Mermilliod, and J. P. Travers, "Quantifying charge carrier localization in chemically doped semiconducting polymers," Phys. Rev. B 53, 4509 (1996).
- ²¹N. W. Ashcroft and N. D. Mermin, *Solid State Physics* (Saunders College, New York, 1976).
- ²²N. F. Mott and E. A. Davis, *Electronic Processes in Non-Crystalline Materials*, 2nd ed. (Oxford University Press, 1979).
- ²³A. J. Epstein, J. Joo, R. S. Kohlman, G. Du, A. G. MacDiarmid, E. J. Oh, Y. Min, J. Tsukamoto, H. Kaneko, and J. P. Pouget, "Inhomogeneous disorder and the modified Drude metallic state of conducting polymers," Synth. Met. 65, 149–157 (1994).
- 24R. Noriega, J. Rivnay, K. Vandewal, F. P. V. Koch, N. Stingelin, P. Smith, M. F. Toney, and A. Salleo, "A general relationship between disorder, aggregation and charge transport in conjugated polymers," Nat. Mater. 12, 1038–1044 (2013)
- ²⁵H. Abdalla, G. Zuo, and M. Kemerink, "Range and energetics of charge hopping in organic semiconductors," Phys. Rev. B 96, 241202(R) (2017).
- 26S. Kang and G. Snyder, "Charge-transport model for conducting polymers," Nat. Mater. 16, 252–257 (2017).

- ²⁷M. Lepinoy, P. Limelette, B. Schmaltz, and F. T. Van, "Thermopower scaling in conducting polymers," Sci. Rep. 10, 8086 (2020).
- 28Y. W. Park, "Structure and morphology: Relation to thermopower properties of conductive polymers," Synth. Met. 45, 173–182 (1991).
- ²⁹A. B. Kaiser, "Systematic conductivity behavior in conducting polymers: Effects of heterogeneous disorder," Adv. Mater. 13, 927–941 (2001).
- ³⁰N. Mateeva, H. Niculescu, J. Schlenoff, and L. R. Testardi, "Correlation of seebeck coefficient and electric conductivity in polyaniline and polypyrrole," J. Appl. Phys. 83, 3111–3117 (1998).
- 31 A. B. Kaiser, "Electronic transport properties of conducting polymers and carbon nanotubes," Rep. Prog. Phys. 64, 1–49 (2000).
- ³²A. M. Glaudell, J. E. Cochran, S. N. Patel, and M. L. Chabinyc, "Impact of the doping method on conductivity and thermopower in semiconducting polythiophenes," Adv. Energy Mater. 5, 1401072 (2014).
 ³³M. N. Gueye, A. Carella, N. Massonnet, E. Yvenou, S. Brenet,
- ³³M. N. Gueye, A. Carella, N. Massonnet, E. Yvenou, S. Brenet, J. Faure-Vincent, S. Pouget, F. Rieutord, H. Okuno, A. Benayad, R. Demadrille, and J. P. Simonato, "Structure and dopant engineering in PEDOT thin films: Practical tools for a dramatic conductivity enhancement," Chem. Mater. 28, 3462–3468 (2016).
- ³⁴P. Limelette, N. Leclerc, and M. Brinkmann, "Heterogeneous oriented structure model of thermoelectric transport in conducting polymers," Sci. Rep. 13, 2116113 (2023).
- ³⁵V. Vijayakumar *et al.*, "Bringing conducting polymers to high order: Toward conductivities beyond $10^5 \, \text{s cm}^{-1}$ and thermoelectric power factors of $2 \, \text{mw m}^{-1} \, \text{k}^{-2}$," Adv. Energy Mater. **9**, 1900266 (2019).
- ³⁶T. Horii, H. Hikawa, M. Katsunuma, and H. Okuzaki, "Synthesis of highly conductive PEDOT:PSS and correlation with hierarchical structure," Polymer 140, 33–38 (2018).
- ³⁷Q. Wei, M. Mukaida, Y. Naitoh, and T. Ishida, "Morphological change and mobility enhancement in PEDOT:PSS by adding co-solvents," Adv. Mater. 25, 2831–2836 (2013).
- ³⁸I. Lee, G. W. Kim, M. Yang, and T. S. Kim, "Simultaneously enhancing the cohesion and electrical conductivity of PEDOT:PSS conductive polymer films using DMSO additives," ACS Appl. Mater. Interfaces 8, 302–310 (2016).
- PEDOT:PSS transparent hole transporting layer with solvent treatment for high performance silicon/organic hybrid solar cells," Nanoscale Res. Lett. 12, 506–514 & (2017)
- ⁴⁰E. Hosseini, V. O. Kollath, and K. Karan, "The key mechanism of conductivity in PEDOT:PSS thin films exposed by anomalous conduction behaviour upon solvent-doping and sulfuric acid post-treatment," J. Mater. Chem. C 8, 3982–3990 (2020).
- ⁴¹Y. Xu, Z. Liu, X. Wei, J. Wu, J. Guo, B. Zhao, H. Wang, S. Chen, and Y. Dou, "Morphological modulation to improve thermoelectric performances of PEDOT: PSS films by DMSO vapor post-treatment," Synth. Met. 271, 116628 (2021).
- ⁴²J. Ouyang, Q. Xu, C. W. Chu, Y. Yang, G. Li, and J. Shinar, "On the mechanism of conductivity enhancement in poly(3,4-ethylenedioxythiophene):poly (styrene sulfonate) film through solvent treatment," Polymer 45, 8443–8450 (2004).
- 43Y. Xia and J. Ouyang, "PEDOT:PSS films with significantly enhanced conductivities induced by preferential solvation with cosolvents and their application in polymer photovoltaic cells," J. Mater. Chem. 21, 4927–4936 (2011).
 44F. Wu, P. Li, K. Sun, Y. Zhou, W. Chen, J. Fu, M. Li, S. Lu, D. Wei, X. Tang,
- ⁴⁴F. Wu, P. Li, K. Sun, Y. Zhou, W. Chen, J. Fu, M. Li, S. Lu, D. Wei, X. Tang, Z. Zang, L. Sun, X. Liu, and J. Ouyang, "Conductivity enhancement of PEDOT: PSS via addition of chloroplatinic acid and its mechanism," Adv. Electron. Mater. 3, 1700047 (2017).
- ⁴⁵J. Nevrela, M. Micjan, M. Novota, S. Kovacova, M. Pavuk, P. Juhasz, J. Kovac Jr., J. Jakabovic, and M. Weis, "Secondary doping in poly (3,4-ethylenedioxythiophene):poly(4-styrenesulfonate) thin films," J. Polym. Sci., Part B: Polym. Phys. 53, 1139–1146 (2015).
- ⁴⁶Z. Guo, T. Sato, Y. Han, N. Takamura, R. Ikeda, T. Miyamoto, N. Kida, M. Ogino, Y. Takahashi, N. Kasuya, S. Watanabe, J. Takeya, Q. Wei, M. Mukaida, and H. Okamoto, "Band transport evidence in PEDOT:PSS films

using broadband optical spectroscopy from terahertz to ultraviolet region," Commun. Mater. 5, 26 (2024).

- ⁴⁷P. G. de Gennes and J. Prost, *The Physics of Liquid Crystals* (Oxford University Press, 1998).
- ⁴⁸D. G. Barci and D. A. Stariolo, "Orientational order in two dimensions from competing interactions at different scales," Phys. Rev. B 79, 075437 (2009).
 ⁴⁹A. M. Nardes, M. Kemerink, R. A. J. Janssen, J. A. M. Bastiaansen,
- ⁴⁹A. M. Nardes, M. Kemerink, R. A. J. Janssen, J. A. M. Bastiaansen, N. M. M. Kiggen, B. M. W. Langeveld, A. J. J. M. van Breemen, and M. M. de Kok, "Microscopic understanding of the anisotropic conductivity of PEDOT:PSS thin films," Adv. Mater. 19, 1196–1200 (2007).
- 50 N. V. Lien and D. D. Toi, "Coulomb correlation effects in variable-range hopping thermopower," Phys. Lett. A 261, 108-113 (1999).
- hopping thermopower," Phys. Lett. A 261, 108–113 (1999).

 ⁵¹K. Behnia, Fundamentals of Thermoelectricity (Oxford University Press, 2015).
- 52J. M. Ziman, Electrons and Phonons (Oxford University Press, 1960).

- ⁵³C. Herring, "Theory of the thermoelectric power of semiconductors," Phys. Rev. 96, 1163–1187 (1954).
- ⁵⁴P. Limelette, M. E. Kamily, H. Aramberri, F. Giovannelli, M. Royo, R. Rurali, I. Monot-Laffez, J. Íñiguez, and G. F. Nataf, "Influence of ferroelastic domain walls on thermal conductivity," Phys. Rev. B 108, 144104 (2023).
- (2023). ⁵⁵T. H. Geballe and G. W. Hull, "Seebeck effect in germanium," Phys. Rev. **94**, 1134–1140 (1954).
- 56Y. Park, Y. Lee, C. Park, L. Shacklette, and R. Baughman, "Thermopower and conductivity of metallic polyaniline," Solid State Commun. 63, 1063–1066 (1987).
- ⁵⁷S. Sakkopoulos, E. Vitoratos, E. Dalas, G. Pandis, and D. Tsamouras, "Thermopower sign reversal versus temperature and DC conductivity in polyaniline derivatives," J. Phys.: Condens. Matter 4, 2231 (1992).